Available online at www.sciencedirect.com
ScienceDirect
International Journal of Thermal Sciences 47 (2008) 1620–1629
International Journal of Thermal Sciences
www.elsevier.com/locate/ijts

Heat transfer study of two-dimensional laminar incompressible offset jet flows

P. Rajesh Kanna [a,b], Manab Kumar Das [b,*]

[a] Department of Mechanical Engineering, National Taiwan University of Science and Technology, Taipei, Taiwan
[b] Department of Mechanical Engineering, Indian Institute of Technology Guwahati, North Guwahati, Guwahati 781039, Assam, India

Received 13 March 2007; received in revised form 29 December 2007; accepted 7 January 2008

Available online 6 February 2008

Abstract

Heat transfer from an isothermal plate by a two-dimensional laminar incompressible offset jet is simulated numerically. The heat transfer characteristics of the jet with respect to offset ratio (*OR*), Reynolds number (*Re*) and Prandtl number (*Pr*) are reported in details. At low *Pr*, conduction mode of heat transfer is dominant in the region. The isotherm is studied inside the recirculation region as well as in the reattachment location. The thermal boundary layer thickness is reduced when *Pr* is increased. Nusselt number is calculated for different *OR* and wide range of *Re* and $Pr = 0.1$, 1 and 100. The variation of the average Nusselt number with different parameters is also reported in details.

Keywords: Laminar heat transfer study; Offset jet; Numerical simulation; Nusselt number

1. Introduction

A jet is defined as a free or bounded one depending upon the distance of the confining boundaries. When the boundaries (parallel to inlet axis) are sufficiently away from the origin of the jet, it is termed as a free jet. A bounded jet will occur when the flow interacts with a parallel wall. This kind of flows occur in many engineering applications such as environmental discharges, heat exchangers, fluid injection systems, cooling of combustion chamber wall in a gas turbine, automobile demister and others. Bounded jets can be classified into three types based on the orientation: (a) impinging jet aimed toward the boundary; (b) wall jet where fluid is discharged at the boundary; and (c) offset jet from a vertical wall of a stagnant pool issuing parallel to a horizontal solid wall.

Fig. 1(a) shows the flow emanating from a two-dimensional (2D) offset jet where the main features and regions of interest are depicted. Due to the entrainment of fluid between the jet and the bottom plate, there is a reduction of pressure in this region forcing the jet to deflect towards the boundary and eventually attach with it. This is called Coanda effect [29]. The offset jet flow has different features in various regions. Within a very short distance from the point of discharge, the jet flow is dominated by momentum and has the properties of a free jet. The flow gets attached when the jet is deflected towards an adjacent solid wall and tends to flow along the boundary. Around the attachment point, that is, the impingement region and part of the recirculation region, it can be partly characterized as an impingement jet. The offset jet has the characteristics of a wall jet in the far field. Other factors which may be important are like free-stream velocity, ambient stratification, buoyancy (density difference), discharge orientation, etc.

Based on the self-similarity solution of the velocity field, analytical solutions of the wall jet are presented by Glauert [13] and Schlichting and Gersten [26]. These solutions are valid only far away from the jet inlet. However, in most applications, the near field development holds the key to important features of the jet flow. Thus, the near field development of a wall jet has been the subject of research in recent years. Schwarz and Caswell [27] have studied the heat transfer characteristics of a 2D laminar incompressible wall jet and presented the exact so-

* Corresponding author. Present address: Department of Mechanical Engineering, Indian Institute of Technology Kharagpur, West Bengal 721302, India.
E-mail addresses: prkanna@gmail.com (P.R. Kanna), manab@mech.iitkgp.ernet.in (M.K. Das).

1290-0729/$ – see front matter
doi:10.1016/j.ijthermalsci.2008.01.003

Nomenclature

h	inlet slot height
H	step height ..... m
i	x-direction grid point
j	y-direction grid point
L	length of the bottom wall ..... m
OR	offset ratio, H/h
n	normal direction
Nu	local Nusselt number
$\overline{Nu}$	average Nusselt number, Eq. (6)
Pr	Prandtl number
Re	Reynolds number, $\bar{U}h/\upsilon$
$\bar{t}$	dimensional time ..... s
t	non-dimensional time
T	dimensional temperature
$\bar{u}, \bar{v}$	dimensional velocity components along $(\bar{x}, \bar{y})$ axes ..... m/s
u, v	dimensionless velocity components along (x, y) axes
$\bar{U}$	inlet mean velocity ..... m/s
$\bar{x}, \bar{y}$	dimensional Cartesian co-ordinates along and normal to the plate ..... m
x, y	dimensionless Cartesian co-ordinates along and normal to the plate
$\Delta x, \Delta y$	grid spacing in x- and y-directions, respectively

Greek symbols

δ	wall jet boundary layer thickness
ε	convergence criterion
θ	dimensionless temperature, $\theta = \frac{T-T_\infty}{T_w-T_\infty}$
κ	clustering parameter
ψ	dimensionless stream function
ω	dimensionless vorticity

Subscripts

max	maximum
w	wall
∞	ambient condition

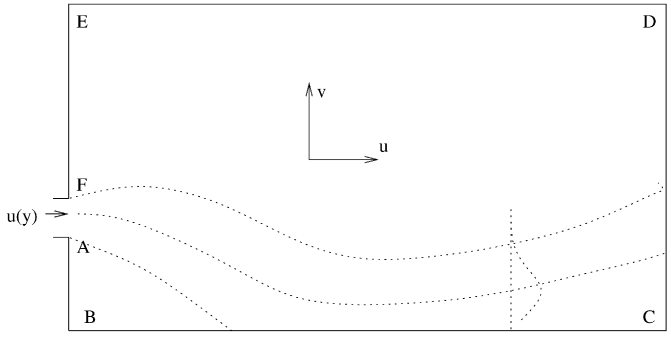

(a) Schematic of the problem

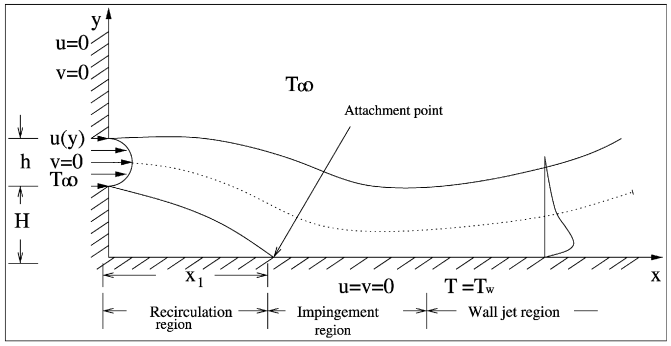

(b) Computational domain

Fig. 1. Schematic diagram and boundary conditions in an offset jet problem.

lutions for both constant wall temperature and constant heat flux cases. In addition, they have solved for variable starting length of the heated section at constant wall temperature. The solution was derived with the plate and jet regimes as non-conjugated. The experimental study on laminar plane wall jet is presented in Bajura and Szewczyk [5] where the jet exit Reynolds number considered is up to $Re = 770$.

Some of the relevant literatures on this subject are by Cohen et al. [8], Amitay and Cohen [3], Quintana et al. [23], Seidel [28]. However, their main aim was to investigate several effects on the transition of wall jet flows. Recently, Bhattacharjee and Loth [6] have simulated the laminar and transitional cold wall jets. They have considered three different inlet profiles viz. parabolic, uniform and ramp and presented the detailed results of time-averaged wall jet thickness and temperature distribution. They have reported that the early transition begins at about $Re = 700$ for plane wall jet.

The 2D incompressible jet development inside a duct in the laminar flow regime for cases with and without entrainment of ambient fluid has been reported by Sarma et al. [25]. Biswas et al. [7] have observed and reported about the evolution of a wall jet-like structure in a three-dimensional backward facing step flow problem. The conjugate heat transfer of a wall jet has been reported by Kanna and Das [17]. The parameter Re, Pr and thermal conductivity ratio are the parameters considered. The laminar plane offset jet flow solution has been presented by Kanna and Das [18]. A comprehensive literature survey may be obtained in this article. The conjugate heat transfer of laminar plane offset jet problem has also been solved by the same authors [19]. The effect of Re, OR and thermal conductivity ratio on the conjugate interface boundary condition and Nu distribution has been presented.

The heat transfer study of a plane laminar offset jet flow is somewhat limited. The effect of an entraining jet located near the jet discharge on the heat transfer, which occurs in several practical applications, has not been studied. In the present study, a time marching incompressible flow solution has been conducted for simulating the heat transfer of an offset jet for a range of offset ratios, Reynolds number and Prandtl number.

2. Mathematical formulation

An incompressible two-dimensional laminar offset jet is considered. For the sake of simplicity, the jet is assumed to be isothermal and having the same density as the ambient fluid. Also, the velocity profile at the jet inlet is taken as parabolic. The step is assumed to be adiabatic condition.

The governing equations for incompressible laminar flow are solved by stream function-vorticity formulation. The transient non-dimensional governing equations in the conservative form are,

Stream function equation

$$\nabla^2\psi = -\omega \tag{1}$$

Vorticity equation

$$\frac{\partial\omega}{\partial t} + \frac{\partial(u\omega)}{\partial x} + \frac{\partial(v\omega)}{\partial y} = \frac{1}{Re}\nabla^2\omega \tag{2}$$

Energy equation

$$\frac{\partial\theta}{\partial t} + \frac{\partial(u\theta)}{\partial x} + \frac{\partial(v\theta)}{\partial y} = \frac{1}{Re\,Pr}\nabla^2\theta \tag{3}$$

where ψ—stream function,

$$u = \frac{\partial\psi}{\partial y}; \qquad v = -\frac{\partial\psi}{\partial x}; \qquad \omega = \frac{\partial v}{\partial x} - \frac{\partial u}{\partial y}$$

The variables are scaled as,

$$u = \frac{\bar{u}}{\bar{U}} v = \frac{\bar{v}}{\bar{U}}; \qquad x = \frac{\bar{x}}{h}; \qquad y = \frac{\bar{y}}{h}$$

$$\omega = \frac{\bar{\omega}}{\bar{U}/h}; \qquad t = \frac{\bar{t}}{h/\bar{U}}, \qquad \theta = \frac{T - T_\infty}{T_w - T_\infty}$$

with the over bar indicating a dimensional variable and $\bar{U}$, h denoting the average jet velocity at nozzle exit and the jet height, respectively.

The boundary conditions needed for the numerical simulation have been prescribed. For an offset jet with entrainment, the following dimensionless conditions have been enforced as shown in Fig. 1(b). The inlet slot height is assumed as, $h = 0.05$ m.

At the jet inlet, along AF (Fig. 1(b)),

$$u(y) = 120y - 2400y^2;$$
$$\omega(y) = 4800y - 120y;$$
$$\psi(y) = 60y^2 - 800y^3 \tag{4a}$$

Along FE, BA and BC, due to no-slip condition,

$$u = v = 0 \tag{4b}$$

Along ED,

$$\frac{\partial u}{\partial y} = 0 \quad \text{and} \quad \frac{\partial v}{\partial y} = 0 \tag{4c}$$

Along BC,

$$\theta = 1 \tag{4d}$$

Along BA and FE adiabatic,

$$\frac{\partial\theta}{\partial x} = 0 \tag{4e}$$

Along FE and ED ambient condition is assumed for θ. At downstream boundary the condition of zero first-derivative has been applied for velocity components. This condition implies that the flow has reached a developed condition. Thus, at CD,

$$\frac{\partial u}{\partial x} = \frac{\partial v}{\partial x} = \frac{\partial\theta}{\partial x} = 0 \tag{4f}$$

Similar type of boundary conditions has been used by Gu [14] and Al-Sanea [1,2].

The Nusselt number and average Nusselt number expressions are given by:

$$Nu(x) = -\left.\frac{\partial\theta}{\partial y}\right|_{y=0} \tag{5}$$

$$\overline{Nu} = \frac{1}{L}\int_0^L Nu(x)\,\mathrm{d}x \tag{6}$$

3. Numerical procedure

The unsteady vorticity transport equation (2) and the energy equation (3) in time are solved by Alternate Direction Implicit scheme (ADI). The central differencing scheme is followed for both the convective as well as the diffusive terms [24]. The details of the discretization procedure are given in Kanna and Das [18].

Thom's vorticity condition has been used to obtain the wall vorticity as given below.

$$\omega_w = -\frac{2(\psi_{w+1} - \psi_w)}{\Delta n^2} \tag{7}$$

where Δn is the grid space normal to the wall. It has been shown by Napolitano et al. [22] and Huang and Wetton [15] that convergence in the boundary vorticity is actually second order for steady problems and for time-dependent problems when $t > 0$. Roache [24] has reported that for a Blasius boundary-layer profile, numerical tests verify that this first-order form is more accurate than the second-order form.

At the bottom wall and the left side wall, constant streamlines are assumed based on inlet flow. At the outlet in the downstream direction, stream-wise gradients are assumed to be zero. At the entrainment boundary, normal velocity gradient is zero [16].

The detailed boundary conditions are,

along FE (Fig. 1(b)),

$$\omega(y) = \frac{2(\psi_w - \psi_{w+1})}{\Delta x_1^2}; \qquad \psi = 0.05 \tag{8a}$$

along BA,

$$\omega(y) = \frac{2(0 - \psi_{w+1})}{\Delta x_1^2}; \qquad \psi = 0 \tag{8b}$$

along BC,

$$\omega(x) = \frac{2(0 - \psi_{w+1})}{\Delta y_1^2}; \qquad \psi = 0 \tag{8c}$$

Solution approaches steady-state asymptotically while time reaches infinity. The computational domain considered here is clustered cartesian grids. For unit length, the grid space at ith node is [21],

$$x_i = \left(\frac{i}{i_{\max}} - \frac{\kappa}{\upsilon}\sin\left(\frac{i\upsilon}{i_{\max}}\right)\right) \tag{9}$$

where υ is the angle and κ is the clustering parameter $\upsilon = 2\pi$ stretches both end of the domain whereas $\upsilon = \pi$ clusters more grid points near one end of the domain. κ varies between 0 to 1. When it approaches 1, more points fall near the end.

The solution of the velocity field is done initially. Details are given in Kanna and Das [18]. Using this velocity field, the energy equation is solved. For the computation, a time step of 0.01 is used for $Pr = 1.0$ and 100.0, whereas for $Pr = 0.01$, time step of 0.0001 is used. The convergence criteria to be set in such a way that it should not terminate at false stage. At steady state, the error reaches the asymptotic behavior. Here it is set as either sum of vorticity error (Eq. (9)) from consecutive time marching steps reduced to the convergence criteria ε or a large total time is elapsed.

$$\sum_{i,j=1}^{i_{\max},j_{\max}} \left(\omega_{i,j}^{t+\Delta t} - \omega_{i,j}^{t}\right) < \varepsilon \tag{10}$$

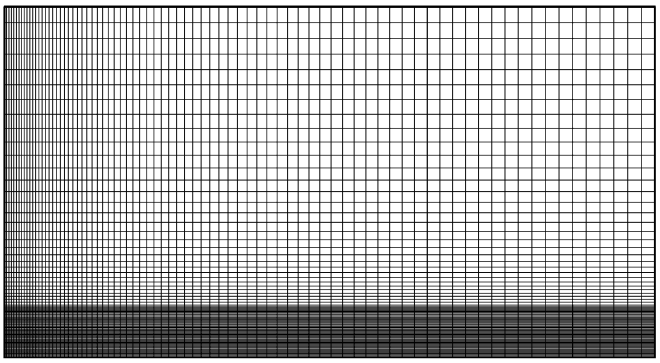

Fig. 2. Typical grids used for offset jet.

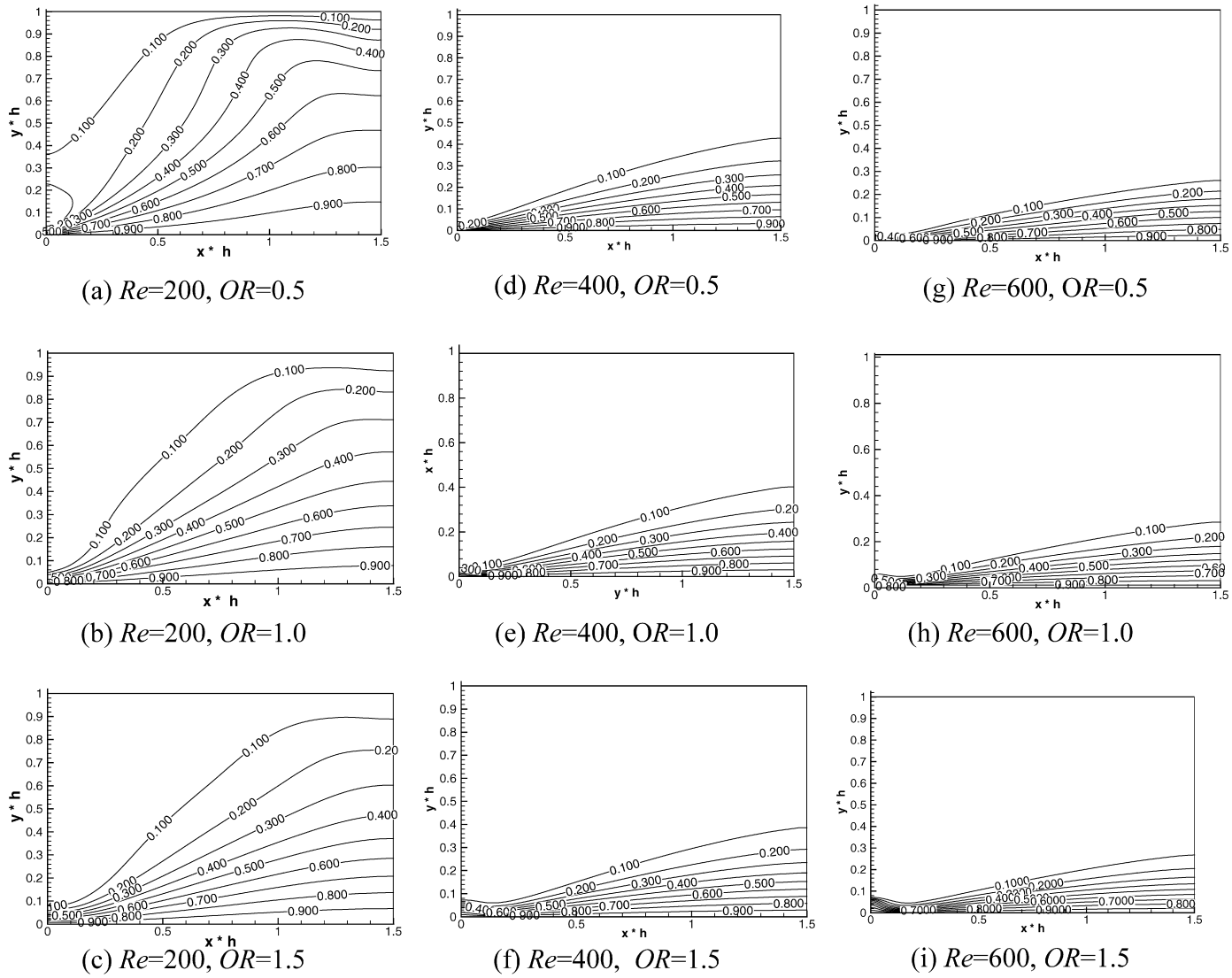

Fig. 3. Effect of offset ratio and Re on isotherm contours, $Pr = 1.0$: (a)–(c) $Re = 200$, (d)–(f) $Re = 400$, (g)–(i) $Re = 600$.

4. Validation of the code

To validate the developed code, the two-dimensional lid-driven square-cavity flow problem [12] and the backward-facing flow problem [4,11] have been solved. Energy equation solution of backward-facing step flow is compared with Dyne and Heinrich [10]. Excellent agreement has been obtained with the benchmark solutions reported in the above references. The laminar plane wall jet problem then has been solved and the computed velocity profiles are compared with the similarity solutions of Glauert [13] and the experimental results of Quintana et al. [23] in a similar way as represented by Seidel [28]. Details are given in Kanna and Das [17,18]. To further validate the code, a plane sudden-expansion flow problem of Durst et al. [9] has been solved. In this case, all the walls except the inlet and the outlet are solid. Thus there is no entrainment from the atmosphere and the boundary conditions are no-slip for these surfaces. Details of the validation results are given in Kanna and Das [18].

5. Grid independence test

The domain has been chosen as $30 \times h$ in streamwise direction and $20 \times h$ in normal direction. Systematic grid refinement study is carried with 51×41, 61×61, 71×61, 81×81 and 101×101 (Fig. 4 of [19]) with $Pr = 1.4$. Grid refinement level 4 is used for the entire computations. The grids are clustered in streamwise direction whereas in normal direction up to $3 \times h$ height, grids are arranged uniformly and above this region, they are clustered. A typical grid is shown in Fig. 2.

6. Results and discussion

The heat transfer study has been carried out with three parameters considered here viz. Re ($\overline{U}h/\upsilon$), Pr and offset ratio (OR). Offset ratio is defined as the ratio of step height (H) to inlet slot height (h). Results are presented here for three OR viz. $OR = 0.5$, 1.0 and 1.5, Re varying from 200 to 600 in steps of 100 and $Pr = 0.01$, 1.0 and 100. The detailed heat transfer results are presented in terms of isotherm contour, Nusselt number and average Nusselt number for these ranges of Re, Pr and OR.

Fig. 3 shows the isotherm lines for all the computed results for $Pr = 1.0$. When $Re = 200$, the isotherms penetrate in the far field region for $OR = 0.5$ (Fig. 3(a)). The diffusion of heat implies that the convection is very small because the amount of entrainment is very small. With increase in OR (Fig. 3(c)) and increase in Re (Fig. 3(f)), the isotherms get concentrated near the wall and convection starts dominating. This is due to the jet spread rate in normal direction is decreased at high Re and OR. When Re is increased to 600 (Figs. 3(g)–7(i)), a depression in the isotherms after the jet exit is noticed. This is due to the reattachment of the jet where recirculation is more and the wall jet boundary layer starts developing. The influence of Pr on isotherms is shown in Fig. 4 for $OR = 1.5$. At low Pr conduction heat transfer is dominant and at high Pr convection is dominant [20]. Fig. 4(a) shows the isotherm of low

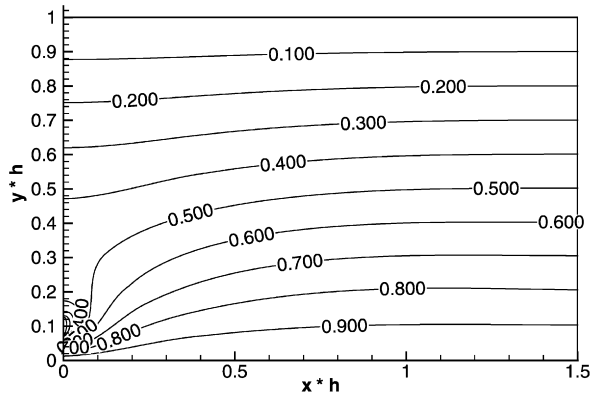

(a) Re=500, Pr=0.01

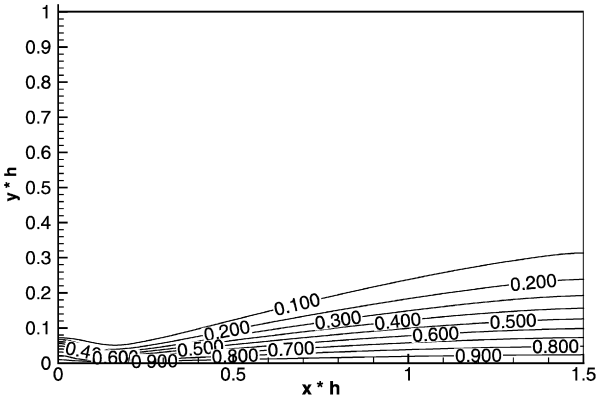

(b) Re=500, Pr=1.0

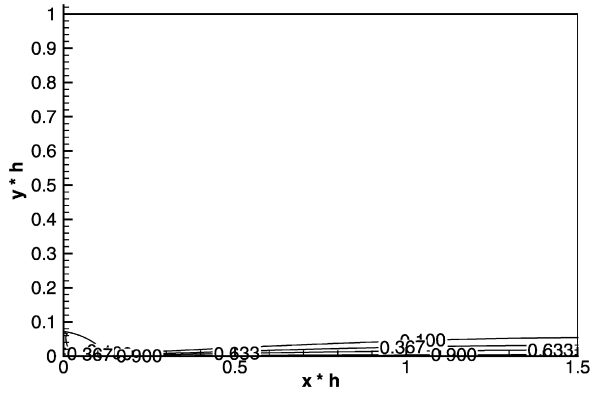

(c) Re=500, Pr=100.0

Fig. 4. Effect of Pr on isotherm contours: $OR = 1.5$.

Pr fluid. Here the heat transfer occurs in the entire solution domain. For the low Pr fluid, conduction is dominant mode of heat transfer and the heat is transferred to the quiescent medium. At $Pr = 100$ (Fig. 4(c)), heat transfer occurs in the thin boundary layer of the main flow where the temperature gradient is high. Fig. 4(b) shows the results for $Pr = 1$.

Non-dimensional temperature distributions at various downstream locations are presented in Fig. 5 (a)–(f). The results are presented for three regions: within recirculation region, at reat-

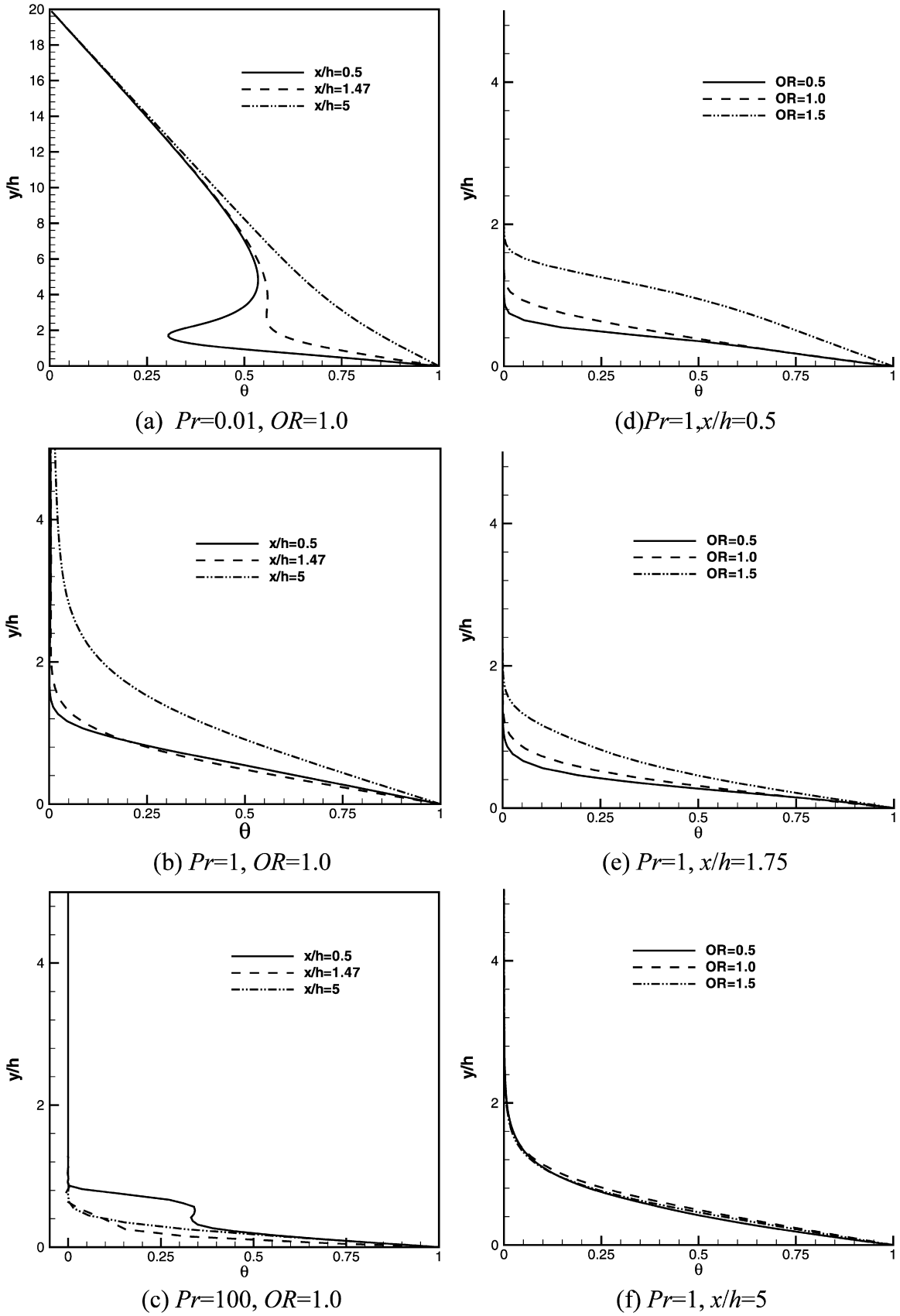

Fig. 5. Temperature distributions at downstream locations: (a)–(c), $Re = 300$, (d)–(f), $Re = 600$.

tachment location and at developing region (Fig. 5 (a)–(c)) for different Pr while OR is kept constant at 1. For low Pr, at $x/h = 0.5$ location, the temperature profile clearly shows the effect of recirculation flow (Fig. 5(a)). A relatively high temperature gradient is obtained because of this effect. At reattachment location and further downstream, the temperature gradient is decreasing. This is due to the flow development and gradual formation of wall jet. For $Pr = 1$, the temperature gradient is maximum at $x/h = 1.47$ (i.e. reattachment location) (Fig. 5(b)). For high Pr (=100), at $x/h = 0.5$, a kink in the temperature contour is observed. Further downstream, at $x/h = 1.47$, maximum temperature gradient is observed. Influence of OR on temperature are shown in Fig. 5 (d)–(f)) for $Re = 600$, $Pr = 1.0$. In recirculation region, when OR is increased, the thermal boundary layer thickness is higher in normal direction. It is noticed that at reattachment location similar trend is existing (Fig. 5(e)). Further downstream location the temperature profile becomes independent of OR (Fig. 5(f)).

Nusselt number is presented in details as a function of Re, Pr and OR. Fig. 6 (a)–(c) shows the influence of Re on Nu with constant $OR = 1.0$. In general when Re is increased, Nu also increases. However, at low Pr this increment is less (Fig. 6(a)). The peak value of Nu occurs at the reattachment location (Fig. 6 (b)–(c)). It shifts in downstream direction when Re is increased since the reattachment length is also increased. Further in the downstream direction, Nu decreases to a near constant value and becomes almost invariant in wall jet region. The effect of Pr is presented in Fig. 7. The Nusselt number gradually increases up to the reattachment location and then onwards, it decreases. This trend is common for any Re and OR. With increase in Pr, the heat transfer from the surface also increases. The effect of OR on Nusselt number is presented in Fig. 8 for $Re = 500$ and different Pr. Near the jet exit due to rapid boundary layer growth, the temperature gradient is larger and results in high Nu (Fig. 8(a)). At $Pr = 1$, the peak Nu decreases significantly for different ORs. The peak value is moved in downstream direction. However it shows less variation at high Pr (Fig. 8(c)).

Maximum Nusselt number for different Re is presented in Fig. 9. Maximum Nusselt number is increased when Re is increased. However it is less sensitive for low Pr. At high Pr it is increased rapidly when Re is increased.

The average Nusselt number for various Re are given in Tables 1–5 in detail. It is noticed that average Nusselt number ($\overline{Nu}$) is increased when Re is increased for particular OR (by comparing the tables). For $Re = 200$ (Table 1), with increase of OR from 0.5 to 1.0, $\overline{Nu}$ decreases whereas it increases when OR is further increased. For $Re = 300$–600 (Tables 2–5), $\overline{Nu}$gradually decreases with increase in OR for $Pr = 0.01$ and 1. However, for $Pr = 100$, $\overline{Nu}$ increases and then decreases with gradual increase in OR. This kind of behavior needs further investigation.

7. Conclusions

Heat transfer study of two-dimensional incompressible non-buoyant offset jet is carried out by solving the momentum equation using stream function and vorticity formulation and the energy equation. Heat transfer characteristics are systematically

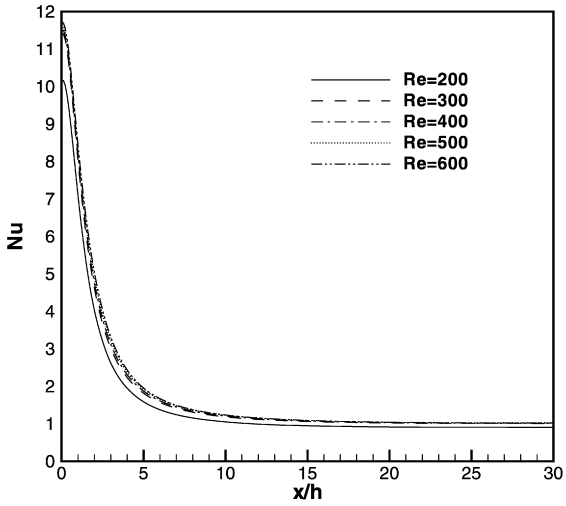

(a) Pr=0.01, OR=1.0

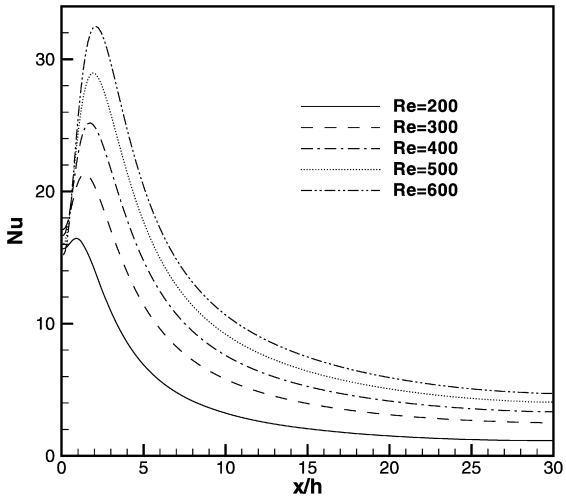

(b) Pr=1.0, OR=1.0

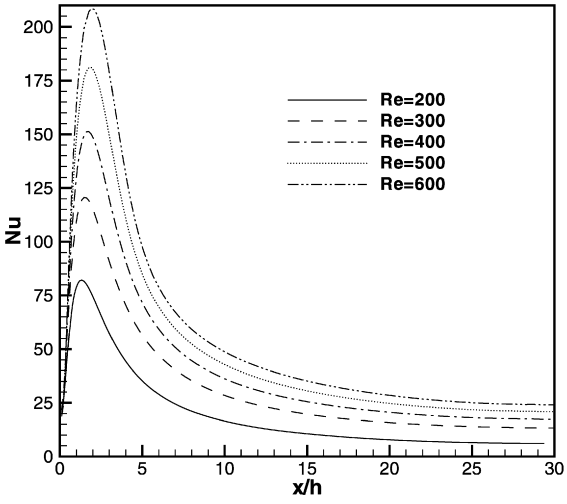

(c) Pr=100.0, OR=1.0

Fig. 6. Nusselt number variation for various Re.

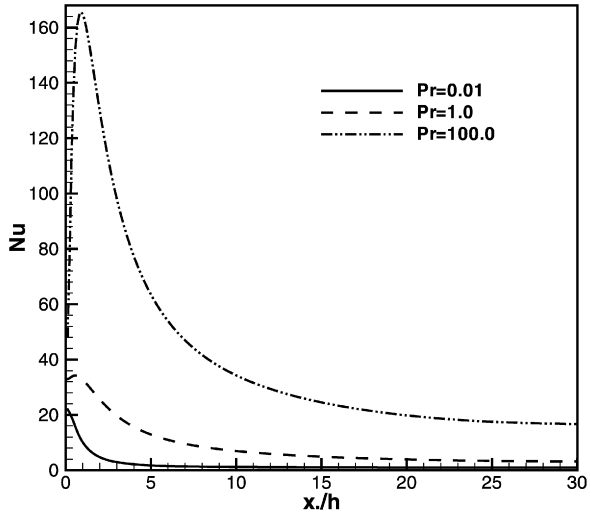

(a) *Re*=400, *OR*=0.5

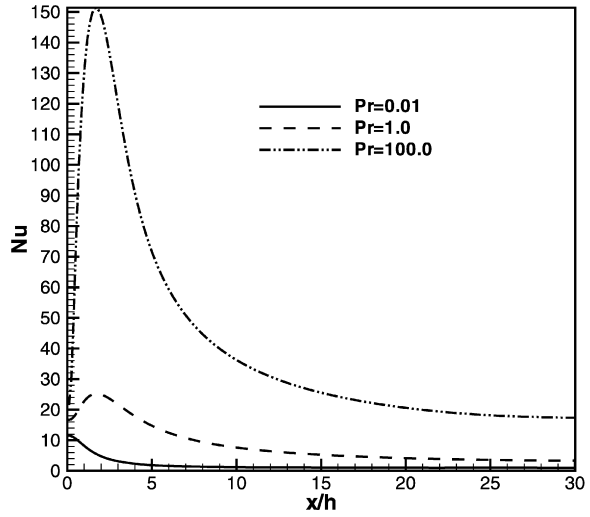

(b) *Re*=400, *OR*=1.0

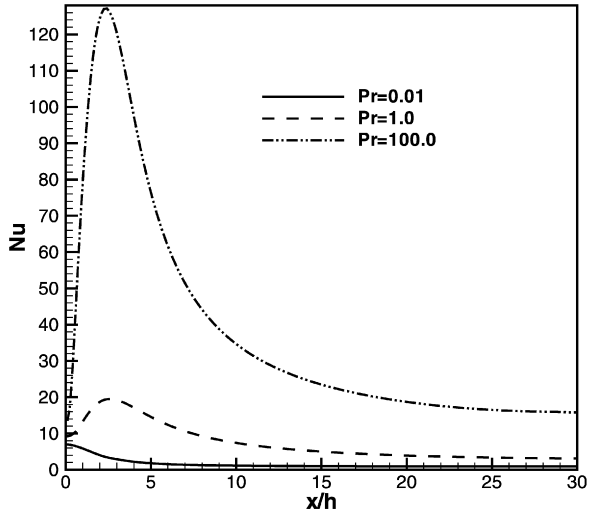

(c) *Re*=400, *OR*=1.5

Fig. 7. Effect of *Pr* on Nusselt number distribution.

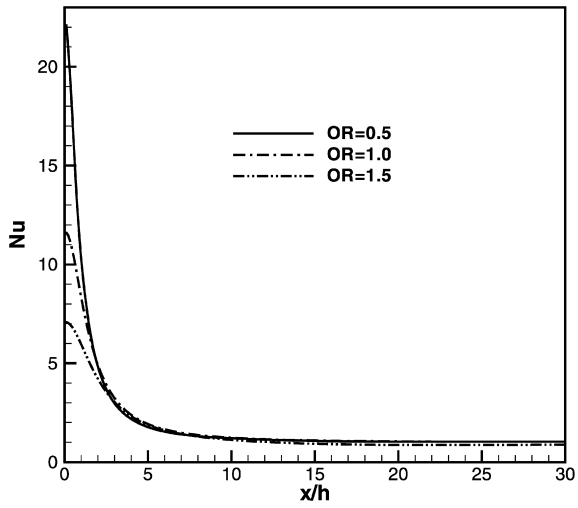

(a) *Pr*=0.01

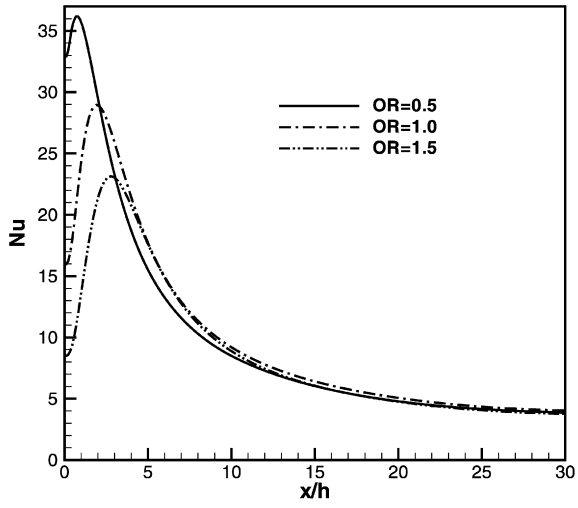

(b) *Pr*=1

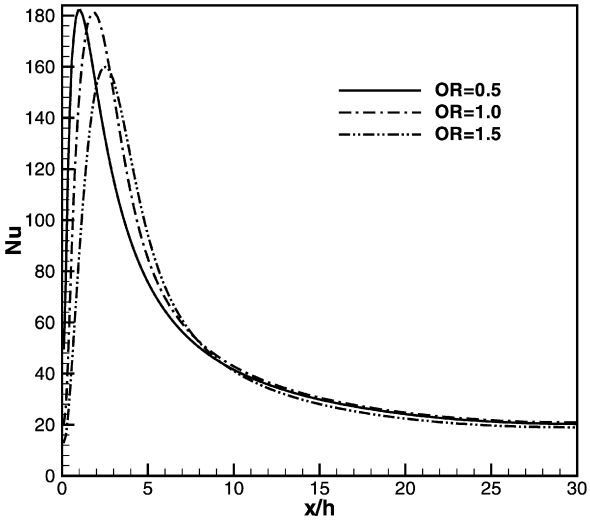

(c) *Pr*=100.0

Fig. 8. Effect of *OR* on Nusselt number: $Re = 500$.

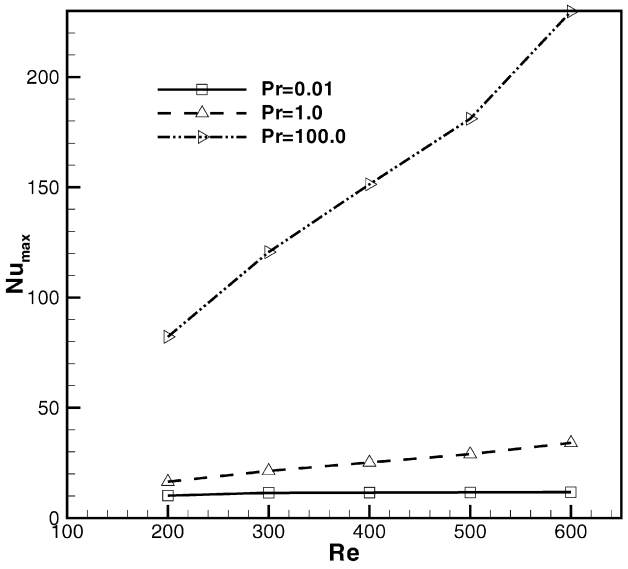

Fig. 9. Maximum Nusselt number. $OR = 1$.

Table 1
Average Nusselt number: $Re = 200$, $L/h = 30$

	$Pr = 0.01$	$Pr = 1.0$	$Pr = 100.0$
$OR = 0.5$	2.82	6.23	28.97
$OR = 1.0$	2.30	5.90	28.84
$OR = 1.5$	2.39	6.43	32.28

Table 2
Average Nusselt number: $Re = 300$, $L/h = 30$

	$Pr = 0.01$	$Pr = 1.0$	$Pr = 100.0$
$OR = 0.5$	2.88	9.79	47.39
$OR = 1.0$	2.59	9.66	48.08
$OR = 1.5$	2.20	8.56	43.52

Table 3
Average Nusselt number: $Re = 400$, $L/h = 30$

	$Pr = 0.01$	$Pr = 1.0$	$Pr = 100.0$
$OR = 0.5$	2.90	12.30	59.57
$OR = 1.0$	2.64	12.18	61.20
$OR = 1.5$	2.25	10.79	56.01

Table 4
Average Nusselt number: $Re = 500$, $L/h = 30$

	$Pr = 0.01$	$Pr = 1.0$	$Pr = 100.0$
$OR = 0.5$	2.98	14.50	70.36
$OR = 1.0$	2.69	14.40	72.95
$OR = 1.5$	2.23	12.77	67.63

studied in detail by varying three parameters viz. *Re*, *Pr* and *OR*. The following conclusions may be drawn.

- For low *Re* and *Pr*, the isotherms penetrate in the far field because conduction effect is high. With increase in *Re*, convection starts dominating which results in concentration of isotherms near the wall.

Table 5
Average Nusselt number: $Re = 600$, $L/h = 30$

	$Pr = 0.01$	$Pr = 1.0$	$Pr = 100.0$
$OR = 0.5$	3.13	20.21	80.10
$OR = 1.0$	2.71	16.37	83.66
$OR = 1.5$	2.33	14.57	78.51

- For same *Re*, increase in *Pr* leads to concentration of isotherms near the wall. At the reattachment points, a significant depression of isotherms are observed implying occurrence of maximum heat transfer.
- In the recirculation region, significant effect on the thermal boundary layer is observed for $Pr = 0.01$ and 100 whereas for $Pr = 1.0$, it is absent.
- For a particular *OR*, there is a remarkable increase in maximum *Nu* with increase in *Pr*. However, it decreases with the increase in *OR*. The relative increase in $Nu_{\max}$ with *Re* is also large for $Pr = 100$ compared to that for $Pr = 0.01$ and 1.
- Average Nusselt number ($\overline{Nu}$) is increased when *Re* and *Pr* are increased. It is decreased when *OR* is increased.

References

[1] S. Al-Sanea, Convection regimes and heat transfer characteristics along a continuously moving heated vertical plate, International Journal of Heat and Fluid Flow 24 (2003) 888–901.
[2] S. Al-Sanea, Mixed convection heat transfer along a continuously moving heated vertical plate with suction or injection, International Journal of Heat and Mass Transfer 47 (2004) 1445–1465.
[3] M. Amitay, J. Cohen, Instability of a two-dimensional plane wall jet, Journal of Fluid Mechanics 344 (1997) 67–94.
[4] B.F. Armaly, F. Durst, J.C.F. Pereira, B. Schonung, Experimental and theoretical investigation of backward-facing step flow, Journal of Fluid Mechanics 127 (1983) 473–496.
[5] R.A. Bajura, A.A. Szewczyk, Experimental investigation of a laminar two-dimensional plane wall jet, Physics of Fluids 13 (1970) 1653–1664.
[6] P. Bhattacharjee, E. Loth, Simulations of laminar and transitional cold wall jets, International Journal of Heat and Fluid Flow 25 (2004) 32–43.
[7] G. Biswas, M. Breuer, F. Durst, Backward-facing step flows for various expansion ratios at low and moderate Reynolds numbers, ASME Journal of Fluids Engineering 126 (2004) 362–374.
[8] J. Cohen, M. Amitay, B.J. Bayly, Laminar-turbulent transition of wall-jet flows subjected to blowing and suction, Physics Fluids 4 (1992) 283–289.
[9] F. Durst, J.C.F. Pereira, C. Tropea, The plane symmetric sudden-expansion flow at low Reynolds numbers, Journal of Fluid Mechanics 248 (1993) 567–581.
[10] B.R. Dyne, J.C. Heinrich, Flow over a backward-facing step: A bench mark problem for laminar flow with heat transfer, Benchmark Problems for Heat Transfer Codes, HTD 222 (1992) 73–76.
[11] D.K. Gartling, A test problem for outflow boundary conditions-flow over a backward-facing step, International Journal for Numerical Methods in Fluids 11 (1990) 953–967.
[12] U. Ghia, K.N. Ghia, C.T. Shin, High *Re* solutions for incompressible flow using the Navier–Stokes equations and multigrid method, Journal of Computational Physics 48 (1982) 387–411.
[13] M.B. Glauert, The wall jet, Journal of Fluid Mechanics 1 (1956) 1–10.
[14] R. Gu, Modelling two-dimensional turbulent offset jets, Journal of Hydraulic Engineering 122 (1996) 617–624.
[15] H. Huang, B.R. Wetton, Discrete compatibility in finite difference methods for viscous incompressible fluid flow, Journal of Computational Physics 126 (1996) 468–478.

[16] S.H. Kang, R. Greif, Flow and heat transfer to a circular cylinder with a hot impinging air jet, International Journal of Heat and Mass Transfer 35 (1992) 2173–2183.

[17] P.R. Kanna, M.K. Das, Conjugate forced convection heat transfer from a flat plate by laminar plane wall jet flow, International Journal of Heat and Mass Transfer 48 (2005) 2896–2910.

[18] P.R. Kanna, M.K. Das, Numerical simulation of two-dimensional laminar incompressible offset jet flows, International Journal for Numerical Methods in Fluids 49 (2005) 439–464.

[19] P.R. Kanna, M.K. Das, Conjugate heat transfer study of two-dimensional laminar incompressible offset jet flows, Numerical Heat Transfer A 48 (2005) 671–691.

[20] T. Kondoh, Y. Nagano, T. Tsuji, Computational study of laminar heat transfer downstream of a backward-facing step, International Journal of Heat and Mass Transfer 36 (1993) 577–591.

[21] R.A. Kuyper, Th.H. Van Der Meer, C.J. Hoogendoorn, R.A.W.M. Henkes, Numerical study of laminar and turbulent natural convection in an inclined square cavity, International Journal of Heat and Mass Transfer 36 (1993) 2899–2911.

[22] M. Napolitano, G. Pascazio, L. Quartapelle, A review of vorticity conditions in the numerical solution of the ζ–ψ equations, Computers and Fluids 28 (1999) 139–185.

[23] D.L. Quintana, M. Amitay, A. Ortega, I.J. Wygnanski, Heat transfer in the forced laminar wall jet, ASME Journal of Heat Transfer 119 (1997) 451–459.

[24] P.J. Roache, Fundamentals of Computational Fluid Dynamics, Hermosa, USA, 1998 (Chapter 3).

[25] A.S.R. Sarma, T. Sundararajan, V. Ramjee, Numerical simulation of confined laminar jet flows, International Journal for Numerical Methods in Fluids 33 (2000) 609–626.

[26] H. Schlichting, K. Gersten, in: Boundary Layer Theory, Springer, 2000, pp. 215–218.

[27] W.H. Schwarz, B. Caswell, Some heat transfer characteristics of the two-dimensional laminar incompressible wall jet, Chemical Engineering Science 16 (1961) 338–351.

[28] J. Seidel, Numerical investigations of forced laminar and turbulent wall jets over a heated surface, PhD thesis, Faculty of the department of Aerospace and Mechanical Engineering. The Graduate College, The University of Arizona, USA, 2001.

[29] D.J. Tritton, in: Physical Fluid Dynamics, Von Norstrand Reinhold, UK, 1977, pp. 284–286.